



1 **Changes in Holocene meridional circulation and poleward Atlantic** 2 **flow: the Bay of Biscay as a nodal point**

3 Mary, Yannick (1), Eynaud, Frédérique (1), Colin, Christophe (2), Rossignol, Linda (1), Brocheray, Sandra (1, 3), Mojtahid,
4 Meryem (4), Garcia, Jennifer (4), Peral, Marion, (1, 5), Howa, H el ene (4), Zaragosi, S ebastien (1), Cremer, Michel (1)

5
6 (1) *Laboratoire Environnements et Pal oenvironnements Oc aniques et Continentaux (EPOC) -UMR 5805, Universit  de*
7 *Bordeaux, 33615 Pessac, France*

8 (2) *Laboratoire G osciences - Universit  de Paris-Sud, 91405 Orsay Cedex, France*

9 (3) *now at: Institut Polytechnique LaSalle-Beauvais – Dpt G osciences, 19 rue Pierre Waguet – BP 30313 – 60026 Beauvais,*
10 *France*

11 (4) *UMR CNRS6112 LPG-BIAF, Recent and Fossil Bio-Indicators, Angers University, 2 Bd Lavoisier, 49045 Angers CEDEX 01,*
12 *France*

13 (5) *now at Laboratoire des Sciences du Climat et de l'Environnement (LSCE-IPSL), Domaine du CNRS, b at.12 - 91198 Gif-sur-*
14 *Yvette, France*

15

16


17 **Keywords**

18 Meridional circulation, Bay of Biscay, Holocene, Sea surface temperature, North Atlantic, Subpolar and

19 Subtropical Gyres

20

21 **Abstract**

22 This paper documents the last 10 ka evolution of one of the key parameters of climate: sea- surface

23 temperatures (SST) in the subpolar North Atlantic. We focus on the southern Bay of Biscay, a **highly**


24 **sensitive oceanographic area because of its strategic and nodal position regarding the dynamics of the**

25 **North Atlantic subpolar and subtropical gyres.** This site furthermore offers unique sedimentary

26 environments characterized by exceptional accumulation rates, enabling the study of Holocene archives at

27 (infra)centennial scales. Our results mainly derive from planktonic foraminiferal association analysis on

28 two cores from the southern Landes plateau. These associations ~~were used as quantitative tools (thanks to~~

29 ~~the Modern Analog Technique)~~ to track  past hydrographical changes. SST reconstructions were thus

30 obtained at an **unprecedented resolution** and compared to a compilation of Holocene records from the



31 northern North Atlantic. From this regional perspective are shown fundamental timing differences


32 between the gyre dynamics, nuancing classical views of a simple meridional overturning cell.



33 1. Introduction

34 **At climatic and shorter meteorological scales**, the key role of the North Atlantic oceanic
35 circulation in climate changes is no longer debatable (e.g., Clark et al., 2002; Bryden et al., 2005). The
36 Atlantic Meridional Overturning Circulation (AMOC) and its dynamics are critical regarding the
37 amplitude and frequency of climate modulations over Europe (westerlies, droughts and/or stormy periods,
38 e.g. Dawson et al., 2007; Magny et al., 2003; Sorrel et al., 2009; Trouet et al., 2012, Van Vliet-Lanoe et
39 al., 2014a and b, Jackson et al., 2015). The two related North Atlantic gyres, the subpolar gyre (SPG) and
40 the subtropical gyre (STG) are fundamental for these processes as they transfer heat and salt toward the
41 Nordic seas (e.g., McCartney and Mauritzen, 2001; Perez-Brunius et al., 2004; Hatun et al., 2005) where
42 convection occurs (e.g. Lozier and Stewart, 2008). Their expansions and contractions notably control the
43 inflow from the North Atlantic Current (NAC) to higher latitudes, thus also affecting the heat budget of
44 the Greenland-Iceland-Norwegian seas, which is critical in the meridional climatic balance (i.e., Hatun et
45 al., 2005, Thornalley et al., 2009). However, complex feedbacks force nonlinear responses within the
46 Earth's radiative budget, preventing climate sciences from providing a precise view of which processes
47 are at play; the incapacity of models to "correctly" represent the last decade of instrumental data is one of
48 the strongest illustrations of this appraisal (e.g., Ba et al., 2014; Karl et al., 2015; Fyfe et al., 2016).

49 During the late Holocene, STG and SPG **latitudinal and/or longitudinal migrations**  contributed to well-
50 known climatic anomalies in Western Europe, such as the Little Ice Age or the Medieval Warm
51 Period/Anomaly, and probably played a major role at longer time scales (Copard et al., 2012; Sorrel et al.,
52 2012; Staines-Urias et al., 2013). By providing the first Holocene inventory of (infra)centennial 

53 hydrographic changes in the inner Bay of Biscay, **this paper aims at testing Western European temperate**
54 **oceanic signals vs. those from a broader North Atlantic view with a focus on the SPG dynamics**, this latter
55 being seen as a key component of the AMOC variability (e.g. Hatun et al., 2005; Thornalley et al., 2009 

56 Colin et al., 2010). Our study site (Figure 1) **is ideally located under the temperate eastern limb of the**
57 **NAC, in the southern Bay of Biscay and close to STG/SPG divergence zone.** This geographic
58 configuration provides to this marine environment a high sensitivity regarding Northern hemisphere
59 climatic signals at present (e.g. Le Cann and Serpette, 2009; Esnaola et al., 2012; Garcia-Soto and




60 Pingree, 2012) with some sedimentary archives furthermore evidencing a strong potential to track down
61 the Holocene variability (Mojtahid et al., 2013; Garcia et al., 2013; Brocheray et al., 2014; Mary et al.,
62 2015),

63 Today, the Bay of Biscay is characterized by a complex, variable sea-surface circulation with
64 strong seasonal changes, marked by a September-October versus March-April - *SOMA* pattern (Pingree
65 and Lecann, 1990; Pingree and Garcia-Soto, 2014). The main surface current in the Bay of Biscay is the
66 European Slope Current (ESC), flowing northward along the Armorican Shelf (Figure 1), with important
67 spatial and seasonal variations (Garcia-Soto and Pingree, 2012; Charria et al., 2013). Circulation can
68 reverse during summer along the shelf break, flowing weakly southwestward (Charria et al., 2013). In
69 autumn-winter, the northward flow reaches a maximum, especially when combining with southern
70 intrusions from the Iberian Poleward Current (IPC) which flows along the western Iberian margin (e.g.
71 Peliz et al., 2005) before turning eastward at the Cape Finisterre (NW Spain). The IPC northward
72 extension into the Bay of Biscay is known as the Navidad Current (e.g. Garcia-Soto et al., 2002; Le Cann
73 and Serpette, 2009). The winter ~~compound of~~ IPC and ESC is designated as the European Poleward
74 Current (EPC, Garcia-Soto and Pingree, 2012), and drives relatively warm and saline water to the Nordic
75 seas, contributing to their heat and salt budget. The Bay of Biscay is additionally strongly marked by
76 surface water inflow coming from the North Atlantic Current (Figure 1), which enters the Bay from its
77 northwestern boundary (Pingree, 2005; Pingree and Garcia-Soto, 2014; Ollitrault and Colin de Verdiere,
78 2014). In contrast with surface circulation of the inner Bay of Biscay, the NAC water inflow shows only
79 limited seasonal variability. At inter-annual time scales however, NAC oscillations are mainly driven by
80 westerly wind regime (Pingree, 2005), and consequently by the North Atlantic Oscillation (NAO), one of
81 the key modes of climatic ~~oscillation~~ in the North Atlantic. So far, little is known about long term
82 oscillations of the NAC inflow into the Bay. Modern surveys of SST variability over the last 150 years in
83 the Bay of Biscay report that temperature oscillations are mainly controlled by the Atlantic Multi-decadal
84 Oscillation (AMO, Garcia-Soto and Pingree, 2012). The influence of the NAO on SST in the Bay of
85 Biscay is more complex and contributes only little to the observed long term trend, although sharp, inter-
86 annual changes of the NAO index impact annual SST variability (Garcia-Soto and Pingree, 2012).



87 Moreover, NAO conditions influence large-scale oceanic circulation patterns indirectly responsible for
88 surface temperature anomalies over the Bay (Pingree, 2005; Garcia-Soto and Pingree, 2012).

89 The present paper is based on analyses conducted on two high-resolution well dated cores from
90 the southern part of the inner Bay of Biscay (Figure 1, Table 1): core KS10b (e.g. Mojtahid et al., 2013)
91 and core PP10-07 (e.g. Brocheray et al., 2014). These cores show exceptionally high sedimentation rates
92 for the Holocene, up to 200 cm.ka⁻¹ for core PP10-07, and 86 cm ka⁻¹ for core KS10b. Here we present
93 reconstructed SST data derived from an ecological transfer function based  the Modern Analogue
94 Technique (see Methods) applied to planktonic *foraminifera* assemblages. **These Bay of Biscay sea-**
95 **surface reconstructions are compared to selected North Atlantic Holocene records onwards a data mining**
96 **exercise done in the frame of the French ANR HAMOC** (Holocene North Atlantic Gyres and
97 Mediterranean Overturning dynamic through Climate Changes) project database (see [http://hamoc-
99 interne.epoc.u-bordeaux1.fr/doku.php?id=start](http://hamoc-
98 interne.epoc.u-bordeaux1.fr/doku.php?id=start)) and referencing sea-surface reconstructions of high time-
100 resolution.

100

101 **2. Methods**


102 **2.1. Age models**

103 Updated age models have been built for the Bay of Biscay cores. All raw ¹⁴C ages were calibrated
104 and converted to calendar ages using the Marine13 calibration curve and the recommended age reservoir
105 of 405 years (Reimer et al., 2013), as no adequate and robust local age reservoir values exist in the area
106 (see Mary et al., 2015 for a discussion). Smooth-spline regression based on the published ¹⁴C dates (n=12
107 for core Ks10b, Mojtahid et al., 2013) were applied (Figure 2). For core PP10-07, two supplementary ¹⁴C
108 dates were obtained at the top of the sequence (Table 2) and the age model was built using a 5 degree
109 polynomial regression (Figure 2). Core MD03-2693 age model (also exploited in this paper) was built
110 using linear interpolation based on published ¹⁴C and ²¹⁰Pb (n=3 and n=8, respectively, Mary et al., 2015).
111 Age-depth modeling and calibration were performed using the dedicated software Clam (Blaauw, 2010),
112 written in the open-source statistical environment R (<http://www.r-project.org/>).



113

114 **2.2.Past hydrographical parameter quantification**

115 Planktonic foraminifera (PF) assemblages were used to quantify sea-surface parameters: species
116 abundances were determined (counts of 300 specimens at least) on the > 150 µm fraction from
117 sedimentary aliquots retrieved at maximum 10 centimeter-intervals along the studied cores, thus giving a
118 mean time resolution of 50 and 150 years for core PP10-07 and KS10b respectively (see Supplementary
119 material for detailed data). SST reconstructions were calculated using the Modern ~~analog technique~~
120 (MAT) a method successfully developed on PF (e.g. Pflaumann et al., 1996; Kucera et al., 2005; Telford
121 and Birks, 2011; Guiot and de Vernal, 2007; 2011). The calculations derive from modern spectra
122 previously compiled and tested separately in the frame of the MARGO exercise for the North Atlantic
123 Ocean and the Mediterranean Sea respectively (Kucera et al., 2005; Hayes et al., 2005). They are based
124 on sediment surface samples analyzed for their contents in PF (specific relative abundances) and thus
125 offer the advantage of already having integrated regional taphonomic processes. At EPOC
126 (Environnements et Paléoenvironnements Océaniques et Continentaux) laboratory, these two MARGO
127 databases were summed to provide larger analog choices and ambiguous data points were excluded (i.e.
128 **undated points**  showing anomalies in the biogeographical distribution), resulting in a final training set of
129 n=1007 modern analogs. Modern sea-surface parameters were extracted from the WOA ATLAS with the
130 sample tool developed by Schäfer-Neth and Manschke (2002). The latter was developed for the MARGO
131 program and interpolates the 10 m World Ocean Atlas WOA -1998 mean seasonal and mean annual
132 temperatures over the four existing data points surrounding the sample location (see [http://www.geo.uni-
134 bremen.de/geomod/staff/csn/woasample.html](http://www.geo.uni-
133 bremen.de/geomod/staff/csn/woasample.html)) thus providing spatio-temporal averaged values of SST
135 considerations).

136 Calculations were run under the R software with the BIOINDIC package (ReconstMAT script) developed
137 by J. Guiot (<https://www.eccorev.fr/spip.php?article389>) using relative abundances of PF with no



138 mathematical transformation (no logarithmic or square root transformations which are frequently used to
139 increase the equitability within assemblages for instance).

140 Past hydrological parameter values are derived from a weighted average of the SST values of the five best
141 analogs. The maximum weight is given for the closest analog in terms of statistical distance (i.e.
142 dissimilarity minimum). The ReconstMAT script furthermore includes the calculation of a threshold
143 regarding this statistical distance which prevents calculation in the case of poor- or ~~no~~ analogous
144 situations. The degree of confidence of this method allows reconstructing seasonal and annual SST with a
145 maximum root mean square error of prediction (RMSEP) of 1.3°C (see Supplementary material). This
146 method (named MATR_1007PF for Modern Analog Technique derived from 1007 modern spectra of PF
147 assemblages) was extensively tested at EPOC including comparisons with similar MAT developed
148 regionally on PF (e.g. Salgueiro et al., 2008; 2010) providing very coherent reconstructions along the
149 western European margin (see Eynaud et al., 2013 for details) and producing pertinent
150 paleoceanographical data (see Penaud et al., 2011; Sánchez Goñi et al., 2012; Sánchez Goñi et al., 2013
151 for records also produced with MATR_1007PF).

152

153 3. Holocene SST oscillations in the Bay of Biscay

154 Despite the different bathymetric and physiographic positions of the studied cores (Figure 1, Table
155 1), reconstructed annual SST in the Bay of Biscay show coherent oscillations of remarkably similar
156 timing (Figure 3a). Small amplitude differences are observed between the two **focused** records, but
157 synchronous warm periods are clearly identified between 8.2-7.4 ka BP and 6.6-5.6 ka BP, these intervals
158 roughly corresponding to the upper and lower limits of the mid-Holocene hypsithermal in the North
159 Atlantic region (e.g. Eynaud et al., 2004; Walker et al., 2012; Tanner et al., 2015).

160 On historical time-scales, warm intervals are detected in both cores between 2.6-1.8 ka BP
161 (Roman Warm Period, RWP) and 1.2-0.5 ka BP (Medieval Warm Period, MWP), although less obvious
162 in core KS10b because of the lower time resolution. An offset of up to 4°C above mean annual modern
163 values is observed during a large temperature excursion around ca 2 Ka BP in core PP10-07 only. The
164 amplitude of the warmings detected between 8.2-7.4 ka BP and 6.6-5.6 ka BP reaches **concomitantly** 2 to



165 3°C in both records. Such amplitudes in the detected SST warm pulses are especially high in comparison
166 to modern annual values. However, considering the strong modern seasonal SST variations in the Bay of
167 Biscay (as shown on Figure 3a), a 4°C shift of mean annual SST is coherent with a deviation of annual
168 mean temperature toward mean summer values.

169 Comparison of the southern Bay of Biscay SST reconstructions with other records from the
170 Western European margin (Figure 3 and 4) suggests that the observed millennial-scaled warm episodes
171 are coherent features which reflect typical climatic patterns, at least expressed regionally, but also
172 probably more broadly. Indeed, further along the Bay of Biscay margin, other high resolution Holocene
173 archives reveal similar and synchronous episodes. Concomitantly to the observed warm SST pulses also
174 seen within the seasonal means (see Supplementary material), Holocene pollen assemblages from core
175 VK03-58 bis (Naughton et al., 2007) indicate a decrease in mean annual precipitations; this drought being
176 related, according to the authors, to a change in the seasonality with warmer summers especially. In the
177 same way, the evolution of coccolithophorid concentrations in the subpolar North-Atlantic along the
178 Irminger Current pathway, interpreted as indicating stronger contribution of NAC water toward the
179 Nordic seas (Andrews and Giraudeau, 2003; Giraudeau et al., 2004, Moros et al., 2012), showed strong
180 similarities with the Bay of Biscay SST signals. Peaks in coccolithophorid abundances in cores B997-330
181 and MD99-2269 (Figure 4e and f) (see location on Figure 1) were recorded synchronously to the warm
182 pulses in the Bay of Biscay, with especially positively marked anomalies detected around 2 ka BP and 8
183 ka BP. The Bay of Biscay SST oscillations further correspond with those reconstructed from marine
184 records from the Barents Shelf (see location on Figure 1) from core MSM5/5-712-2 (Werner et al., 2013,
185 Figure 3c) and core M23258 (Sarnthein et al., 2003; Figure 3d). This coherency suggests teleconnections
186 between the southern Bay of Biscay and the Nordic seas, probably due to a common driving mechanism
187 linked to the NAC inflow vigor and to the modulation of its split off Ireland between the SPG and the
188 STG.

189 In between the observed warm intervals, SST reconstructions of core PP10-07 and KS10b reveal
190 several low values slightly colder than today (Figure 3a). The time interval between 5.6 and 2.6 ka BP is
191 characterized by temperatures around -1°C compared to the modern ones. This period roughly



192 corresponds to the late Holocene Neoglacial Cooling (e.g. Eynaud et al., 2004; Wanner et al., 2008;
193 Walker et al., 2012). In the same way, short-lived events of 2°C cooling are visible around ca 8.2, 7, 4,
194 2.9 and 1.7 ka BP (Figure 3 and 4). The two older anomalies are synchronous and well-marked in both
195 KS10b and PP10-07 cores.

196 The comparison of the timing of these cold spells to other existing Holocene reconstructions from
197 the North Atlantic Ocean reveals that they represent coherent and reproducible features (Figure 4).
198 Interestingly, density anomalies thought to reflect millennial-scale variability in the SPG dynamics
199 (Thornalley et al., 2009; Farmer et al., 2011) were synchronously recorded at sub-thermocline depths in
200 the southern Iceland basin. These anomalies were interpreted as reflecting a strong /*weak*, longitudinally
201 extended/*contracted* SPG thus driving more/*less* vigorous but fresher/*saltier* Atlantic inflow throughout
202 the Faroe current branch and thus modulating the AMOC strength (Thornalley et al., 2009). The good
203 temporal correspondence between the cold spells detected in core PP10-07 (even if shorter) and the
204 density anomalies (core RAPID-12-1K, Figure 4h) registered in the subpolar North-Atlantic support, as
205 seen for warm events, a direct teleconnection with the inner Bay of Biscay, probably throughout a
206 STG/SPG seesaw which would influence tracks/intensities of the temperate westerlies. The short lived
207 cold anomalies of PP10-07 are furthermore concomitant with periods of increased storminess identified in
208 various coastal sediments from the NW European margin (Holocene Storm Periods after Sorrel et al.,
209 2012, Figure 3g). These periods have been related to a weakened, westward contracted SPG, involving a
210 rapid feedback in the atmospheric dynamics.

211 In the subtropical North Atlantic, study of benthic foraminiferal stable isotopes in core EUGC-3B
212 (located in the Galician Shelf, Pena et al., 2010; see Figure 1) also showed similar cold anomalies which
213 were interpreted by the authors as suggesting enhanced contribution of colder, NE Atlantic ENACW
214 waters reaching the Iberian margin during these events.

215



216 **4. The European poleward current and the influence of subtropical sourced**
217 **waters in the Bay of Biscay**

218 Modern surveys (e.g. Garcia-Soto et al., 2002; Lozier and Stewart, 2008; Garcia-Soto and Pingree,
219 2012) and paleoceanographic time-series (e.g., Mojtahid et al., 2013) recently evidenced the influence of the
220 IPC, and its extension in the Bay of Biscay (i.e. Navidad Current, Garcia-Soto et al., 2002), on surface
221 circulation and hydrological conditions along the European Margin. At present, these incursions of warm
222 waters in the bay occur during winter under specific seasonal wind regimes (of southerly wind off Portugal
223 and westerly wind off Northern Spain, Charria et al., 2013) and negative anomalies of sea level pressure
224 over the North Atlantic (Pingree and Garcia-Soto, 2014). While these conditions were previously related to a
225 negative mode of the NAO (Garcia-Soto et al., 2002), recent analysis of instrumental time-series showed
226 that weather conditions responsible for Navidad current may not always correspond to a fixed value of the
227 NAO index (Pingree and Garcia-Soto, 2014). The Navidad Current occasionally creates warm SST
228 anomalies, enhanced transport of warm water through the pole and could thus be the vector of planktonic
229 exotic (from subtropical origin) faunal invasions in the inner Bay of Biscay (see Mojtahid et al., 2013 and
230 Garcia et al., 2013 for example in the fossil record; see Garcia-Soto and Pingree, 2012 and Pingree and
231 Garcia-Soto, 2014 for example in instrumental time-series) which could bias our SST reconstructions. In the
232 following, we thus examine the hypothesis of a persistent poleward surface current during the Holocene that
233 would have triggered the observed SST warm anomalies in the PP10-07 and KS10b records.

234 In order to test the coherency of surface hydrographic features along the temperate and subtropical adjacent
235 portions of the European margin, we compared Bay of Biscay SST reconstructions with existing SST
236 (annual) records produced along the Iberian Margin (Figure 3b and c). We first test this link over historical
237 times, compiling SST high resolution data obtained on the proximal core MD03-2693 (after Mary et al.,
238 2015), which matches accurately those from core PP10-07 (see Figure 3a between 0.5 and 1.5 ka and also
239 Figure E4 in the Supplementary material), with additional high resolution records (Figure 3b). The
240 combination of these records reveals a slight warming associated to the Medieval Warm Period and coherent
241 low-amplitude multi-decadal SST oscillations which echoes those of AMO anomalies as reconstructed by
242 Mann et al (2009). Especially striking is the high degree of synchronicity detected between the Iberian



243 margin (core PO287-06, Abrantes et al., 2011) and the Bay of Biscay at the scale of the last 1.5 ka, despite
244 differences in the proxies used to generate paleo-SST (Alkenones vs MAT on PF respectively) and age-
245 model uncertainties (which probably explain offsets of a few hundred years around 1200 A.D.). The good
246 coherency with AMO reconstructions further supports modern oceanographic assumptions of AMO driving
247 multi-decadal change of SST in the area (Garcia-Soto and Pingree, 2012) and shows that this modulation is
248 at least valid for the late Holocene. Interestingly, modern winter incursions of Iberian water through the Bay
249 of Biscay take place during periods of increasing AMO (Garcia-Soto and Pingree, 2012). During these
250 episodes, warm winter anomalies of up to 1.1° are observed in the Bay of Biscay, which are consistent with
251 the amplitude of the warmings detected in both MD03-2693 and PP10-07 past reconstructions.

252 However, ~~at a longest~~ Holocene perspective, existing SST records from the Iberian margin do not
253 reveal any coherent patterns with those from the Bay of Biscay over the last 10 ka (Figure 3C).
254 Regardless of the proxies involved in SST reconstructions (Alkenones and MAT), there is no evidence of
255 any earlier distinct SST excursions in the high time resolution data of the Iberian cores MD99-2331,
256 D13882, MD95-2042 and MD01-2444 (Figure 3c, see also Figure E4 in the Supplementary material) or
257 elsewhere in other lower resolution Holocene records from the same area (Naughton et al., 2007; Martrat
258 et al., 2007; Rodrigues et al., 2009; Voelker and de Abreu, 2011; Chabaud et al., 2014). The early
259 Holocene SST reconstructions in this area show a monotonous long term decrease of SST correlated with
260 the Holocene decline of summer insolation (e.g. Marchal et al., 2002, see also Figure E4) which contrasts
261 strongly with the warm episodes observed in core PP10-07 and KS10b at that time (see Figure E4 in the
262 Supplementary material). Taking into account the similarities between late Holocene records in the
263 Iberian margin and in the Bay of Biscay, our data thus suggests a disconnection between these two
264 regions during the first part of the Holocene, up to 1.5 ka BP. We interpret this divergence as a distinct
265 response of the Bay of Biscay to North Atlantic millennial changes in the NAC/SPF system dynamics
266 (e.g. Perez-Brunius et al., 2004) whereas southwestern Europe has probably undergone a mixed influence
267 of diverse subtropical climatic trends. Sea-surface environments from the Bay of Biscay, located at the
268 interface between the SPG and STG influences may have, as currently observed in frontal regions,
269 recorded an amplified signature of NAC shifts, themselves driven by contraction/extension phases of the



270 whole North-Atlantic gyre system (STP, SPG, and Polar Gyre also). To decipher the role of each of these
271 gyres is at present not possible on the basis of our records only, and requires additional high-resolution
272 comparable marine archives along a latitudinal gradient at least between 30° and 60°N. The analyses of
273 the influence of Mediterranean hydrographic changes (via the Mediterranean outflow export especially)
274 together with those linked to the Eastern North Atlantic Upwelling Region would also be very important
275 to tackle in such a context.

276

277 **5. Implication for Holocene climate dynamics**

278 In agreement with modern climate observations (e.g. Ba et al., 2014), North Atlantic paleoceanographic
279 studies describe a strong impact of the Subpolar gyre (SPG) dynamics on the NAC inflow toward high-
280 latitudes and global circulation during the Holocene (Bianchi and Mc Cave, 1999; Oppo et al., 2003;
281 Perez-Brunius et al., 2004; Thornalley et al., 2009; Giraudeau et al., 2010; Moros et al., 2012; Staines-
282 Urías, 2013). Freshwater fluxes in the Labrador Sea and wind stress over the North Atlantic are key
283 drivers of eastern extensions/contractions of the SPG (Hatun et al., 2015), thus also controlling the
284 salinity balance over the North Atlantic, boreal deep-water convection and North hemisphere climate
285 patterns. The compilation of proxy-records from further south in the Bay of Biscay indicates that the
286 Holocene relatively long-term periods of warming ~~in the Bay of Biscay~~ are interbedded/superposed to
287 rapid, millennial cold anomalies of SPG origin (Figure 4). In agreement with other North Atlantic
288 records, strong NAC occurs preferentially during the Holocene optimum (Berner et al., 2007; Solignac et
289 al., 2008), and during the Roman Warm Period (Werner et al., 2012). In contrast, the occurrences of cold
290 anomalies in the North Atlantic follow a 1500 years periodicity during the Holocene (e.g., Thornalley et
291 al., 2009; Debret et al., 2007; Sorrel et al., 2012), and are accurately reflected by the SST PP10-07 record
292 (Figure 4f).

293 As also suggested by recent studies of modern time-series (Lozier et al., 2010; Lozier, 2012), Holocene
294 SST records from the Bay of Biscay evidence a decoupling of gyre dynamics, and a potential gyre-
295 specific expression of the AMOC. Model studies similarly question the meridional coherence of the



296 AMOC, revealing an inherent character of its mid-latitude variability at decadal time-scales (Bingham et
297 al., 2007), mainly driven by wind forcing and eddy variability. While our findings support coherent sea-
298 surface hydrographical patterns between subtropical and temperate environments along the western
299 European margin, suggesting a coupled SPG/STG gyre dynamics over the last 1.5 to 2 ka, earlier
300 Holocene contexts seem to have been rather favorable to a gyre-specific expression, as seen at least from
301 SST reconstructions. To understand climatic processes behind these observations and test their coherency
302 region per region, a pan-(North)-Atlantic view is required, urging for comprehensive data compilation
303 efforts as those undertaken for instance in the work conducted for the Ocean2k SST synthesis (e.g.
304 McGregor et al., 2015). SST records should however been incremented by complementary parameters
305 when possible, especially to document hydrographic processes at various depth, in order to better
306 understand the 3D articulation of the oceanic thermal and dynamic responses to various Holocene
307 forcings (e.g. changes in insolation, sea-level - gateway connection, volcanism, or even anthropogenic
308 related, which could have been cumulative or not).

309

310 6. Conclusion

311 Our study, which documents Holocene surface hydrographical changes at unprecedented time-
312 scales in the Bay of Biscay, reveals contrasted patterns which accurately reflect the variability of the
313 North Atlantic gyre dynamics. Coherently with stronger NAC inflow in the Nordics seas as detected in
314 other archives from the northern North Atlantic, our high-resolution sedimentary records identify specific
315 warm periods during the early Holocene and at ca. 2 ka BP and reveal that northward advection of
316 subtropical waters may have influenced SST oscillations in the Bay of Biscay during the last 1.5 ka BP.
317 In addition, SST signals from the Bay of Biscay show the occurrences of short-term cold anomalies,
318 interpreted here as the signature of changes in SPG dynamics. The influence of the two main North
319 Atlantic gyres, i.e STP vs SPG, observed asynchronously over most of the Holocene in the Bay of Biscay,
320 indicate fundamental differences in the temporal variability of their dynamics, contrasting with the idea of
321 a coherent, basin-wide-driven, overturning cell in the North-Atlantic. Our results suggest a gyre-specific



322 expression of the AMOC, which may contribute to strong regionalisms in the response of the North

323 Atlantic hydrography to Holocene climatic changes.

324

325 7. Acknowledgments

326 Analyses documented in this study have been supported by the French ANR HAMOC. We are
327 grateful to the captain and crew of the RV *Pourquoi Pas?* and to the scientific team of the 2010-
328 SARGASS cruise. This work benefited from ¹⁴C AMS measurement facilities thanks to the ARTEMIS
329 French project. We thank Giovanni Sgubin, Didier Swingedouw and Eleanor Georgiadis for useful
330 discussions and comments on the manuscript. This is an UMR EPOC contribution. Data will be set on
331 <http://www.pangaea.de/>.

332

333 M.Y. and E.F. designed the study and wrote the paper in the frame of the ANR HAMOC project
334 coordinated by C.C..

335 E.F., R.L., M.M., G.J., P.M., H.H. performed and/ or supervised planktonic foraminifera assemblage
336 analyses and picking for the datings. E.F. ran the transfer function. M.Y. performed age modelling with
337 the help of E.F. and M.M.. B.S, S.Z. and C.M. investigated the sedimentology of core PP10-07. All
338 authors contributed to discussions and interpretation of the results. The authors declare no competing
339 financial interests.

340



341 8. References

342 Abrantes, F., Rodrigues, T., Montanari, B., Santos, C., Witt, L., Lopes, C. and Voelker, A.: Climate of
343 the last millennium at the southern pole of the North Atlantic Oscillation: an inner-shelf sediment record of
344 flooding and upwelling, *Climate Research* 48, 261–280, doi:10.3354/cr01010, 2011. - *Data available from*
345 *<http://doi.pangaea.de/10.1594/PANGAEA.761849>*.

346 Andrews, J.T. and Giraudeau, J.: Multi-proxy records showing significant Holocene environmental
347 variability: the inner N. Iceland shelf (Hunafloi), *Quaternary Science Reviews* 22, 175–193, 2003.

348 Ba, J., Keenlyside, N. S., Latif, M., Park, W., Ding, H., Lohmann, K., Mignot, J., Menary, M., Otterå,
349 O. H., Wouters, B., Salas y Melia, D., Oka, A., Bellucci, A., and Volodin, E.: A multi-model comparison of
350 Atlantic multidecadal variability, *Climate Dynamics* 43, 2333–2348, 2014.

351 Berner, K.S., Koç, N., Godtlielsen F., and Divine, D.: Holocene climate variability of the Norwegian
352 Atlantic Current during high and low solar insolation forcing, *Paleoceanography* 26, n/a–n/a., 2011.

353 Bianchi, G.G. and Mc Cave, I.N.: Holocene periodicity in North Atlantic climate and deep-ocean flow
354 south of Iceland, *Nature* 397, 515–517, 1999.

355 Bingham, R.J., Hughes, C.W., Roussenov, V., and Williams R.G.: Meridional coherence of the North
356 Atlantic meridional overturning circulation. *Geophysical Research Letters* 34, n/a–n/a. 2007.

357 Blaauw, M.: Methods and code for 'classical' age-modelling of radiocarbon sequences, *Quaternary*
358 *Geochronology* 5, 512–518, 2010.

359 Brocheray, S., Cremer, M., Zaragosi, S., Schmidt, S., Eynaud, F., Rossignol L., and Gillet, H.: 2000
360 years of frequent turbidite activity in the Capbreton Canyon (Bay of Biscay), *Marine Geology*, 347, 136–
361 152, doi:10.1016/j.margeo.2013.11.009, 2014.

362 Bryden, H. L., Longworth, H. R., and Cunningham, S. A.: Slowing of the Atlantic meridional
363 overturning circulation at 25° N, *Nature* 438, 655–657, 2005.

364 Chabaud, L., Sanchez Goni, M.F., Desprat, S., and Rossignol, L.: Land-sea climatic variability in the
365 eastern North Atlantic subtropical region over the last 14,200 years: Atmospheric and oceanic processes at
366 different timescales, *The Holocene* 24, 787–797, 2014.



- 367 Charria, G., Lazure, P., Le Cann, B., Serpette, A., Reverdin, G., Louazel, S., Batifoulier, F., Dumas,
368 F., Pichon, A., and Morel Y.: Surface layer circulation derived from Lagrangian drifters in the Bay of
369 Biscay, *Journal of Marine Systems* 109-110, S60–S76. doi:10.1016/j.jmarsys.2011.09.015, 2013.
- 370 Clark, P.U., Pisias, N.G., Stocker, T.F., and Weaver A.J.: The role of the thermohaline circulation in
371 abrupt climate change, *Nature* 415, 863–869, 2002.
- 372 Copard, K., Colin, C., Henderson, G.M., Scholten, J., Douville, E., Sicre, M.-A., and Frank, N.: Late
373 Holocene intermediate water variability in the northeastern Atlantic as recorded by deep-sea corals, *Earth
374 and Planetary Science Letters*, 313-314, 34–44. doi:10.1016/j.epsl.2011.09.047, 2012.
- 375 Debret, M., Bout-Roumazielle, V., Grousset, F., Desmet, M., McManus, J. F., Massei, N., Sebag, D.,
376 Petit, J.-R., Copard, Y., and Trentesaux A.: The origin of the 1500-year climate cycles in Holocene North-
377 Atlantic records. *Climate of the Past* 3, 569–575, 2007.
- 378 Esnaola, G., Sáenz, J., Zorita, E., Fontán, A., Valencia, V., and Lazure, P.: Daily scale winter-time sea
379 surface temperature variability and the Iberian Poleward Current in the southern Bay of Biscay from 1981 to
380 2010. *Ocean Science Discussions* 9, 3795–3850, 2012.
- 381 Eynaud, F., Turon, J.L., and Duprat, J.: Comparison of the Holocene and Eemian palaeoenvironments
382 in the South Icelandic Basin: Dinoflagellate cysts as proxies for the North Atlantic surface circulation,
383 *Review of Palaeobotany and Palynology*, 128, 55–79, 2004.
- 384 Eynaud, F., Malaizé, B., Zaragosi, S., de Vernal, A., Scourse, J., Pujol, C., Cortijo, E., Grousset, F.E.
385 Penaud, A., Toucanne, S., Turon, J.-L. and Auffret, G.: New constraints on European glacial freshwater
386 releases to the North Atlantic Ocean, *Geophysical Research Letters*, 39(15). L15601, 2012.
- 387 Farmer, E.J., Chapman, M.R., and Andrews, J.E.: Holocene temperature evolution of the subpolar
388 North Atlantic recorded in the Mg/Ca ratios of surface and thermocline dwelling planktonic foraminifers,
389 *Global and Planetary Change*, 79, 234–243, 2011.
- 390 Garcia, J., Mojtahid, M., Howa, H., Michel, E., Schiebel, R., Charbonnier, C., Anschutz, P., and
391 Jorissen F.J.: Benthic and planktic foraminifera as indicators of late glacial to Holocene paleoclimatic
392 changes in a marginal environment: An example from the southeastern Bay of Biscay, *Acta Protozool*, 52,
393 163–182, 2013.



- 394 Garcia-Soto, C., Pingree, R. D., and Valdés, L.: Navidad development in the southern Bay of Biscay:
395 Climate change and swoddy structure from remote sensing and in situ measurements, *Journal of*
396 *Geophysical Research*, 107, 2002.
- 397 Garcia-Soto, C. and Pingree, R.D.: Atlantic Multidecadal Oscillation (AMO) and sea surface
398 temperature in the Bay of Biscay and adjacent regions, *Journal of the Marine Biological Association of the*
399 *United Kingdom*, 92, 213–234, 2012.
- 400 Gaudin, M, Mulder, T., Cirac, P., Berne, S., and Imbert P.: Past and present sedimentation activity in
401 the Capbreton Canyon, southern Bay of Biscay, *Geo-Marine Letters* 26, 331–345, 2006.
- 402 Giraudeau, J., Jennings, A. E., and Andrews, J.T.: Timing and mechanisms of surface and intermediate
403 water circulation changes in the Nordic Seas over the last 10,000 cal years: a view from the North Iceland
404 shelf, *Quaternary Science Reviews*, 23, 2127–2139, 2004.
- 405 Giraudeau, J., Grelaud, M., Solignac, S., Andrews, J.T., Moros, M., and Jansen, E.: Millennial-scale
406 variability in Atlantic water advection to the Nordic Seas derived from Holocene coccolith concentration
407 records, *Quaternary Science Reviews*, 29, 1276–1287. doi:10.1016/j.quascirev.2010.02.014, 2010.
- 408 Guiot, J. and de Vernal, A.: Transfer functions: Methods for quantitative paleoceanography based on
409 microfossils. In: Hillaire-Marcel C. and de Vernal A. (eds), *Proxies in Late Cenozoic Paleocanography*,
410 Amsterdam: Elsevier, pp. 523–563, 2007.
- 411 Guiot, J. and de Vernal A.: Is spatial autocorrelation introducing biases in the apparent accuracy of
412 paleoclimatic reconstructions?, *Quaternary Science Reviews*, 30, 1965–1972, 2011.
- 413 Hatun, H., Britt Sandø, A., Drange, H., Hansen, B. and Valdimarsson, H.: Influence of the Atlantic
414 Subpolar Gyre on the Thermohaline Circulation, *Science*, 309, 1841–1844, 2005.
- 415 Hayes, A., Kucera, M., Kallel, N., Saffi, L. and Rohling, E. J.: Glacial Mediterranean sea surface
416 temperatures based on planktonic foraminiferal assemblages, *Quaternary Science Reviews*, 24, 999–1016,
417 2005.
- 418 Jackson, L.C., Kahana, R., Graham, T., Ringer, M. A., Woollings, T., Mecking, J. V., and Wood, R.
419 A.: Global and European climate impacts of a slowdown of the AMOC in a high resolution GCM, *Clim*
420 *Dyn*, 1–18, doi:10.1007/s00382-015-2540-2, 2015.



421 Kennett, J.R., Allen, M., Beer, J., Grootes, P., Laj, C., McManus, J., and Ramesh, R.: Decadal-to-
422 millennial-scale climate variability—chronology and mechanisms: summary and recommendations,
423 Quaternary Science Reviews 21, 1121–1128, 2002.

424 Kucera, M., Weinelt, M., Kiefer, T., Pflaumann, U., Hayes, A., Weinelt, M., Chen, M.-T., Mix, A.-C.,
425 Barrows, T.T., Cortijo, E., Duprat, J., Juggins, S., and Waelbroeck, C.: Reconstruction of sea-surface
426 temperatures from assemblages of planktonic foraminifera: multi-technique approach based on
427 geographically constrained calibration data sets and its application to glacial Atlantic and Pacific Oceans,
428 Quaternary Science Reviews, 24, 951–998, doi:10.1016/j.quascirev.2004.07.014, 2005.

429 Le Cann, B., and Serpette, A.: Intense warm and saline upper ocean inflow in the southern Bay of
430 Biscay in autumn–winter 2006–2007, Continental Shelf Research, 29, 1014–1025,
431 doi:10.1016/j.csr.2008.11.015, 2009.

432 Lherminier, P., and Thierry, V.: The Reykjanes Ridge Experiment, <http://wwz.ifremer.fr>, 2015.

433 Lozier, M.S. and Stewart, N. M., On the Temporally Varying Northward Penetration of Mediterranean
434 Overflow Water and Eastward Penetration of Labrador Sea Water, Journal of Physical Oceanography, 38,
435 2097–2103, 2008.

436 Lozier, M.S., Roussenov, V., Reed, M.S.C. and Williams, R.G.: Opposing decadal changes for the
437 North Atlantic meridional overturning circulation, Nature Geoscience 3, 728–734, 2010.

438 Lozier, M.S.: Overturning in the North Atlantic, Annual Review of Marine Science 4, 291–315, 2012.

439 Magny, M, Bégeot, C, Guiot, J. et al. Contrasting patterns of hydrological changes in Europe in
440 response to Holocene climate cooling phases, Quaternary Science Reviews, 22, 1589–1596, 2003.

441 Mann, M.E., Zhang, Z., Rutherford, S., Bradley, R. S., Hughes, M. K., Shindell, D., Ammann, C.
442 Faluvegi, G. and Ni F.: Global signatures and dynamical origins of the Little Ice Age and Medieval Climate
443 Anomaly, Science, 326: 1256–1260, 2009. *Data available from*
444 http://www.meteo.psu.edu/holocene/public_html/supplements/MultiproxySpatial09/

445 Marchal, O., Cacho, I., Stocker, T.F., Grimalt, J.O., Calvo, E., Martrat, B., Shackleton, N., Vautravers,
446 M., Cortijo, E. and van Kreveld S.: Apparent long-term cooling of the sea surface in the northeast Atlantic
447 and Mediterranean during the Holocene, Quaternary Science Reviews, 21, 455–483, 2002.



- 448 Martrat, B., Grimalt, J.O., Shackleton, N.J., de Abreu, L., Hutterli, M.A. and Stocker, T. F.: Four
449 Climate Cycles of Recurring Deep and Surface Water Destabilizations on the Iberian Margin. *Science* 317,
450 502–507. *Data available from* <http://doi.pangaea.de/10.1594/PANGAEA.771894>, 2007.
- 451 Mary, Y., Eynaud, F., Zaragosi, S., Malaizé, B., Cremer, M. and Schmidt, S.: High frequency
452 environmental changes and deposition processes in a 2 kyr-long sedimentological record from the Cap-
453 Breton canyon (Bay of Biscay), *The Holocene*, 25, 348–365, doi:10.1177/0959683614558647, 2015.
- 454 Mojtahid, M., Jorissen, F.J., Garcia, J., Schiebel, R., Michel, E., Eynaud, F., Gillet, H., Cremer, M.,
455 Diz Ferreiro, P., Siccha, M., and Howa, H.: High resolution Holocene record in the southeastern Bay of
456 Biscay: Global versus regional climate signals, *Palaeogeography, Palaeoclimatology, Palaeoecology*, 377,
457 28–44. doi:10.1016/j.palaeo.2013.03.004, 2013.
- 458 McCartney, M.S., and Mauritzen, C.: On the origin of the warm inflow to the Nordic Seas, *Progress in*
459 *Oceanography*, 51, 125–214, 2001.
- 460 McGregor, H.V., Evans, M.N., Goosse, H., Leduc, G., Martrat, B., Addison, J.A., Mortyn, P.G., Oppo,
461 D.W., Seidenkrantz, M.-S., Sicre, M.-A., Phipps, S.J., Selvaraj, K., Thirumalai, K., Filipsson, H.L., Ersek,
462 V.: Robust global ocean cooling trend for the pre-industrial Common Era. *Nature Geoscience* 8, 671–677.
463 doi:10.1038/ngeo2510, 2015.
- 464 Moros, M., Jansen, E., Oppo, D.W., Giraudeau, J., and Kuijpers, A.: Reconstruction of the late-
465 Holocene changes in the Sub-Arctic Front position at the Reykjanes Ridge, north Atlantic, *The Holocene*,
466 22, 877–868, 2012.
- 467 Naughton, F., Bourillet, J.F., Sanchez Goni, M.-F., Turon J.-L., and Jouanneau J.-M.: Long-term and
468 millennial-scale climate variability in northwestern France during the last 8850 years, *The Holocene*, 17,
469 939–953, 2007a.
- 470 Naughton, F., Sanchez Goñi, M.F., Desprat, S., Turon, J.-L., Duprat, J., Malaizé, B., Joli, C., Cortijo,
471 E., Drago T. and Freitas, M.C.: Present-day and past (last 25000 years) marine pollen signal off western
472 Iberia, *Marine Micropaleontology*, 62, 91–114, doi:10.1016/j.marmicro.2006.07.006, 2007b.
- 473 Ollitrault, M. and Colin de Verdière A.: The ocean general circulation near 1000 m depth, *J. Phys.*
474 *Oceanogr.* 44, 384–409, 2014.



- 475 Peliz, Á., Dubert, J., Santos, A.M.P., Oliveira, P.B., Le Cann, B.: Winter upper ocean circulation in the
476 Western Iberian Basin—Fronts, Eddies and Poleward Flows: an overview, *Deep Sea Research Part I:*
477 *Oceanographic Research Papers*, 52, 621–646, doi:10.1016/j.dsr.2004.11.005, 2005.
- 478 Pena, L.D., Francés, G., Diz, P., Esparza, M., Grimalt, J.O., Nombela, M.A. and Alejo, I.: Climate
479 fluctuations during the Holocene in NW Iberia: High and low latitude linkages, *Continental Shelf Research*,
480 30, 1487–1496, doi:10.1016/j.csr.2010.05, 2010.
- 481 Penaud, A., Eynaud, F., Sánchez-Goñi, M.F., Malaizé, B., Turon, J.L., and Rossignol L.: Contrasting
482 sea-surface responses between the western Mediterranean Sea and eastern subtropical latitudes of the North
483 Atlantic during abrupt climatic events of MIS 3, *Marine Micropaleontology*, 80, 1-17, 2011.
- 484 Pérez-Brunius, P., Rossby, T., Watts, D.R.: Absolute transports of mass and temperature for the North
485 Atlantic Current-Subpolar Front system, *Journal of physical oceanography*, 34, 1870–1883, 2004.
- 486 Pflaumann, U., Duprat, J., Pujol, C., and Labeyrie, L. D.: SIMMAX: A modern analog technique to
487 deduce Atlantic sea surface temperatures from planktonic foraminifera in deep-sea sediments,
488 *Paleoceanography*, 11, 15–35, 1996.
- 489 Pingree, R.: North Atlantic and North Sea climate change: curl up, shut down, NAO and ocean colour,
490 *Journal of the Marine Biological Association of the United Kingdom*, 85, 1301–1315, 2005.
- 491 Pingree, R. D. and Garcia-Soto, C.: Plankton blooms, ocean circulation and the European slope
492 current: Response to weather and climate in the Bay of Biscay and W English Channel (NE Atlantic), *Deep*
493 *Sea Research Part II: Topical Studies in Oceanography*, 106, 5–22, 2014
- 494 Pingree, R.D. and Le Cann B.: Structure, strength and seasonality of the slope currents in the Bay of
495 Biscay region, *Journal of the Marine Biological Association of the United Kingdom*, 70, 857–885, 1990.
- 496 Reimer, P.J., Bard, E., Bayliss, A., Beck, J. W., Blackwell, P. G., Ramsey, C. B., Buck, C. E., Cheng,
497 H., Edwards, R. L., Friedrich, M., Grootes, P. M., Guilderson, T. P., Haflidason, H., Hajdas, I., Hatté, C.,
498 Heaton, T. J., Hoffmann, D. L., Hogg, A. G., Hughen, K. A., Kaiser, K. F., Kromer, B., Manning, S. W.,
499 Niu, M., Reimer, R. W., Richards, D. A., Scott, E. M., Southon, J. R., Staff, R. A., Turney, C. S. M. and
500 van der Plicht, J.: IntCal13 and Marine13 Radiocarbon Age Calibration Curves 0-50,000 Years cal BP,
501 *Radiocarbon*, 55(4), 2013.



- 502 Rodrigues, T., Grimalt, J.O., Abrantes, F.G., Flores, J.A. and Lebreiro, S.M., (Holocene
503 interdependences of changes in sea surface temperature, productivity, and fluvial inputs in the Iberian
504 continental shelf (Tagus mud patch), *Geochemistry, Geophysics, Geosystems* 10, n/a–n/a.
505 doi:10.1029/2008GC002367, 2009. *Data available from* <http://doi.pangaea.de/10.1594/PANGAEA.761812>
- 506 Salgueiro, E., Voelker, A., Abrantes, F., Meggers, H., Pflaumann, U., Loncaric, N., González-
507 Álvarez, R., Oliveira, P., Bartels-Jänsdättr, H.B., Moreno, J. and Wefer, G.: Planktonic foraminifera
508 from modern sediments reflect upwelling patterns off Iberia: Insights from a regional transfer function,
509 *Marine Micropaleontology* 66, 135–164, 2008.
- 510 Salgueiro, E., Voelker, A.H.L., de Abreu, L., Abrantes, F., Meggers, H., Wefer, G.: Temperature and
511 productivity changes off the western Iberian margin during the last 150 ky, *Quaternary Science Reviews*
512 29, 680–695, 2010.
- 513 Sánchez Goñi, M.F, Bakker, P., Desprat, S., Carlson, A. E., Van Meerbeeck, C. J., Peyron, O.,
514 Naughton, F., Fletcher, W. J., Eynaud, F., Rossignol, L. and Renssen, H.: European climate optimum and
515 enhanced Greenland melt during the Last Interglacial, *Geology*, 40, 627-630, 2012.
- 516 Sánchez Goñi, M.F., Bard, E., Landais, A., Rossignol, L., d’Errico, F.: Air–sea temperature
517 decoupling in western Europe during the last interglacial–glacial transition, *Nature Geoscience* 6, 837-841,
518 doi:10.1038/ngeo1924, 2013.
- 519 Sarnthein M., Van Kreveld, S., Erlenkeuser, H., Grootes, P. M., Kucera, M., Pflaumann, U., Schulz,
520 M.: Centennial-to-millennial-scale periodicities of Holocene climate and sediment injections off the western
521 Barents shelf, 75°N, *Boreas*, 32, 447–461. doi:10.1080/03009480310003351, 2003.
- 522 Schäfer-Neth, C. and Manschke, A., WOA-Sample tool, [http://www.geo.uni-](http://www.geo.uni-bremen.de/geomod/staff/csn/woasample.html)
523 [bremen.de/geomod/staff/csn/woasample.html](http://www.geo.uni-bremen.de/geomod/staff/csn/woasample.html), 2002. last access: January 2016.
- 524 Staines-Urías, F., Kuijpers, A., and Korte, C.: Evolution of subpolar North Atlantic surface circulation
525 since the early Holocene inferred from planktic foraminifera faunal and stable isotope records. *Quaternary*
526 *Science Reviews* 76, 66–81, 2013.



- 527 Solignac, S., Grelaud, M., de Vernal, A., Giraudeau, J., Moros, M., McCave N. and Hoogakker, B.:
528 Reorganization of the upper ocean circulation in the mid-Holocene in the Northeastern Atlantic, Can. J.
529 Earth Sci. 45, 1417-1433, 2008.
- 530 Sorrel, P., Debret, M., Billeaud I., Jaccard S.L., McManus J.F., and Tessier B.: Persistent non-solar
531 forcing of Holocene storm dynamics in coastal sedimentary archives, Nature Geoscience 12, 892–896.
532 doi:10.1038/ngeo1619, 2012.
- 533 Tanner, B.R., Lane, C.S., Martin, E.M., Young, R. and Collins, B.: Sedimentary proxy evidence of a
534 mid-Holocene hypsithermal event in the location of a current warming hole, North Carolina, USA.
535 Quaternary Research 83, 315–323. doi:10.1016/j.yqres.2014.11.004, 2015.
- 536 Telford, R.J. and Birks, H.J.B.: Effect of uneven sampling along an environmental gradient on
537 transfer-function performance, Journal of Paleolimnology 46, 99–106, 2011.
- 538 Telford, R. J., Li, C., and Kucera M.: Mismatch between the depth habitat of planktonic foraminifera
539 and the calibration depth of SST transfer functions may bias reconstructions, Climate of the Past, 9, 859-
540 870, 2013.
- 541 Thornalley, D. J. R., Elderfield, H. and McCave, I.N.: Holocene oscillations in temperature and
542 salinity of the surface subpolar North Atlantic, Nature 457, 711–714, 2009.
- 543 Trouet V., Scourse, J.D. and Raible, C.C.: North Atlantic storminess and Atlantic Meridional
544 Overturning Circulation during the last Millennium: Reconciling contradictory proxy records of NAO
545 variability, Global and Planetary Change, 84–85, 48-55, 2012.
- 546 Van Vliet-Lanoe, B., Goslin, J., Hallegouet, B., Henaff, A., Delacourt, C., Fernane, A., Franzetti, M.,
547 Le Cornec, E., Le Roy, P., Penaud, A.: Middle- to late-Holocene storminess in Brittany (NW France): Part I
548 - morphological impact and stratigraphical record, The Holocene, 24, 413–433,
549 doi:10.1177/0959683613519687, 2014a.
- 550 Van Vliet-Lanoe, B., Penaud, A., Henaff, A., Delacourt, C., Fernane, A., Goslin, J., Hallegouet, B., Le
551 Cornec, E.: Middle- to late-Holocene storminess in Brittany (NW France): Part II - The chronology of
552 events and climate forcing, The Holocene, 24, 434–453, doi:10.1177/0959683613519688, 2014b.



553 Voelker, A.H.L., de Abreu, L.: A Review of Abrupt Climate Change Events in the Northeastern
554 Atlantic Ocean (Iberian Margin): Latitudinal, Longitudinal, and Vertical Gradients, in: Rashid, H., Polyak,
555 L., Mosley-Thompson, E. (Eds.), Geophysical Monograph Series. American Geophysical Union,
556 Washington, D. C., pp. 15–37, 2011.

557 Wanner, H., Beer J., Bütikofer J., Crowley T.J., Cubasch U., J. Flückiger, H. Goosse, M. Grosjean, F.
558 Joos, J.O. Kaplan, M. Küttel, S.A. Müller, Prentice I.C., Solomina O., Stocker T.F., Tarasov P., Wagner M.
559 and Widmann M.: Mid- to Late Holocene climate change: an overview, Quaternary Science Reviews 27,
560 1791–1828. doi:10.1016/j.quascirev.2008.06.013, 2008.

561 Walker, M. J. C., Berkelhammer, M., Björck, S., Cwynar, L. C., Fisher, D. A., Long, A. J., Lowe, J. J.,
562 Newnham, R. M., Rasmussen S. O., and Weiss, H.: Formal subdivision of the Holocene Series/Epoch: a
563 Discussion Paper by a Working Group of INTIMATE (Integration of ice-core, marine and terrestrial
564 records) and the Subcommission on Quaternary Stratigraphy (International Commission on Stratigraphy),
565 Journal of Quaternary Science, 27, 649–659, 2012.

566 Werner, K., Spielhagen, R.F., Bauch, D., Hass, H.C. and Kandiano, E.S.: Atlantic Water advection
567 versus sea-ice advances in the eastern Fram Strait during the last 9 ka: Multiproxy evidence for a two-phase
568 Holocene, Paleoceanography, 28(2), 283-295, Data available from
569 <http://doi.pangaea.de/10.1594/PANGAEA.810415>, 2013.

570



571

572 **Table caption**

573

574 **Table 1:** Location and references of the southern Bay of Biscay cores used in this study.

575

576 **Table 2:** Summary of AMS ^{14}C ages of core PP10-07 with calendar correspondences.

577



578

Cruise, Core label	Latitude (°N)	Longitude (°E)	Water depth (m)	Longitudinal distance (km) from the shore	Datasources and references
SARGASS, PP10-07	43.677	-2.228	1472	58	This work , Brocheray et al., 2014
PROSECAN IV, KS10b	43.833	-2.050	550	50	This work , Mojtahid et al., 2013
SEDICAR/PICABIA, MD03-2693	43.654	-1.663	431	15	This work , Gaudin et al., 2007, Mary et al., 2015

579

Table 1: Location and references of the southern Bay of Biscay cores used in this study.

580

581

582

583

Depth in core PP10-07 (cm)	Sample	Material	Ref Number	mg C	d ¹³ C	pMC corrected			RAW 14C Age yr BP			corrected reservoir age / -400 yr BP	Calibrated age CLAM yr BP	-2σ yr	+2σ yr	Error yr	Confidence %
						±	0,24	±	±	±	±						
4,5	PP10-07, 3-6 cm (TR1)	Bulk planktonic foraminifera	SacA39103	0,572	0,12	90,6	±	0,24	790	±	30	390	423	353	493	70	92,6
124,5	PP10-07 124-125 cm (TR2)	Bulk planktonic foraminifera	SacA39104	0,455	-1,1	82,1	±	0,24	1590	±	30	1190	1149,5	1063	1236	86,5	95
219,5	PP10-07 218-221	Bulk planktonic foraminifera	SacA 29590	0,7	0,2	77,5	±	0,19	2050	±	30	1650	1618	1533	1702	85	95
380	PP10-07 / 380	Bulk planktonic foraminifera	SacA 26975	0,78	-4,6	72,2	±	0,24	2615	±	30	2215	2271	2175	2366	96	95
720,5	PP10-07 / 720-721	Bulk planktonic foraminifera	SacA 26976	1	-0,9	58,8	±	0,22	4265	±	30	3865	4380	4272	4487	108	95
1050	PP10-07 / 1050	Bulk planktonic foraminifera	SacA 26977	1,1	-5,2	49,4	±	0,17	5660	±	30	5260	6070	5970	6170	100	95
1180	PP10-07 1180	Bulk planktonic foraminifera	SacA 29591	0,69	-0,3	44,6	±	0,14	6490	±	30	6090	7007	6897	7116	110	95
1540	PP10-07 / 1537-1543	Bulk planktonic foraminifera	SacA 26978	1,17	-1,9	33,8	±	0,17	8705	±	40	8305	9371	9276	9466	95	95
1731,5	PP10-07 1730-1733	Bulk planktonic foraminifera	SacA 29592	0,84	-0,8	33	±	0,12	8900	±	30	8500	9556	9477	9635	79	95
1981,5	PP10-07 1980-1983	Bulk planktonic foraminifera	SacA 29593	1	-1,5	31,6	±	0,12	9270	±	30	8870	10093	9992	10193	101	92

584

585

Table 2: Summary of AMS ¹⁴C ages of core PP10-07 with calendar correspondences.

586

587 **Figure caption**

588 **Figure 1:** A) map showing the regional scheme of the main surface currents in the Bay of
589 Biscay, drawn after the compilation of modern hydrological survey from Pingree and Garcia-
590 Soto (2014). North Atlantic Current (NAC), Iberian poleward Current (IPC), and European
591 Slope Current (ESC) are respectively represented by the red and orange arrows. The studied
592 sedimentary cores PP10-07 and KS10b from the inner Bay of Biscay are shown in red.
593 Additional Holocene records cited in the text are displayed by green squares. B) North
594 Atlantic general circulation pattern (SPG: Subpolar Gyre, STG: Subtropical Gyre, EPC:
595 European Poleward Current, after Lherminier and Thierry, 2015) with the location of the
596 northern and southern sedimentary records discussed in the text. Core references: **1**-Brocheray
597 et al., 2014; **2**-Mojtahid et al., 2013; **3**-Gaudin et al., 2006; Mary et al., 2015; **4**-Naughton et
598 al., 2007a; **5**-Pena et al., 2010; **6**-Werner et al., 2013; **7**-Sarnthein et al., 2003; **8**-Giraudeau et
599 al., 2004; **9**-Andrews and Giraudeau, 2003; **10**-Thornalley et al., 2009; **11**- Naughton et al.,
600 2007b; **12**-Abrantes et al., 2011; **13**-Chabaud et al., 2014; **14**- Rodrigues et al., 2009; **15**-
601 Martrat et al., 2007.

602

603 **Figure 2:** Revised age models for cores KS10b, MD03-2693, and PP10-07 (left panels)
604 compared to previous published age models (right panels with original references).

605

606 **Figure 3:** Mean Annual sea surface temperature (SST) records from the Western European
607 margin. A) Holocene SST signals from cores PP10-07 and KS10b (this study) reconstructed
608 using the Modern Analog Technique (MAT) based on planktonic foraminifera (see Methods),
609 and compared to SST signal of the adjacent core MD03-2693 (Mary et al., 2015). Black dots
610 identify ^{14}C age control points. B) SST signals spanning the last 1500 years in the Bay of
611 Biscay (core MD03-2693) based on MAT and from the Iberian Margin (core PO287-06,



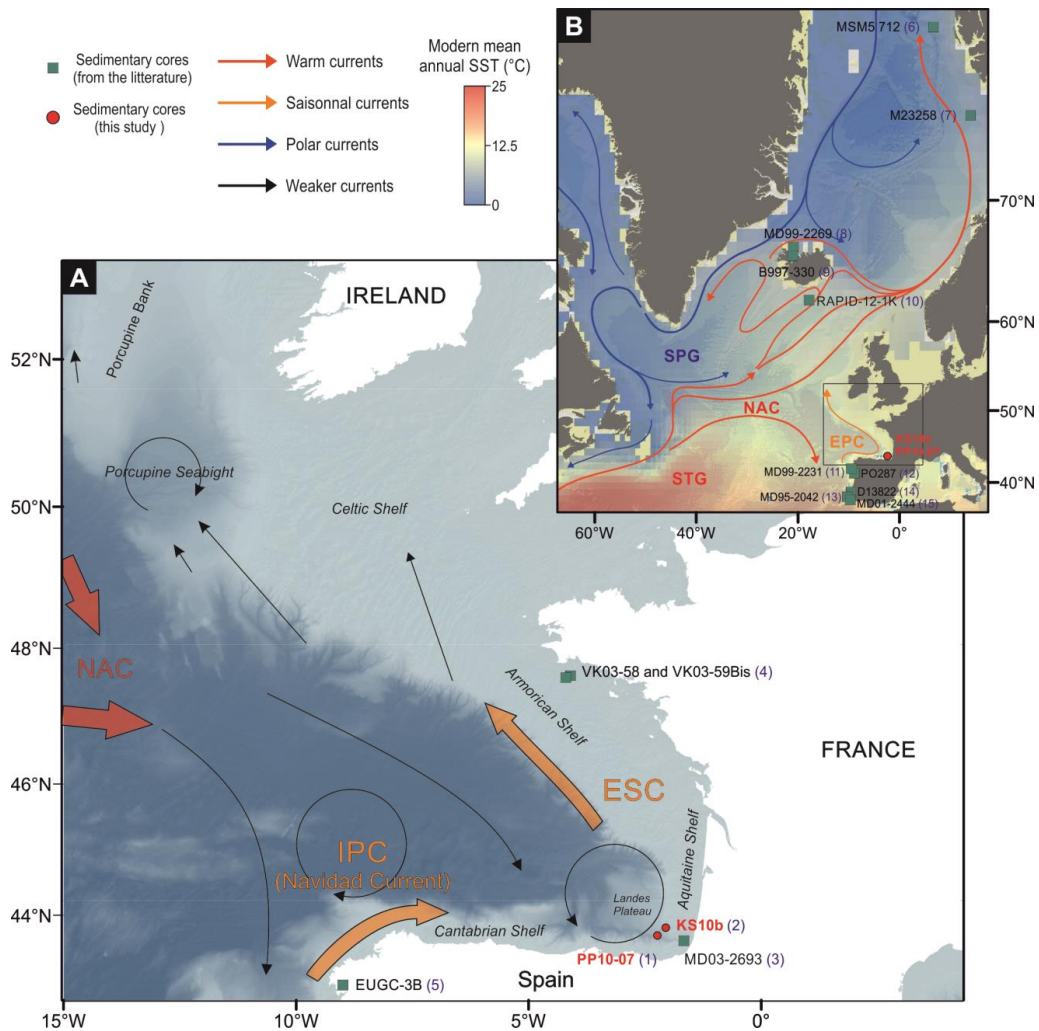
612 Abrantes et al., 2011) using alkenones. Reconstructed signals are compared with the AMO
613 reconstruction of Mann et al., (2009). The dotted curve represents core MD03-2693 signal
614 transposed on top of the two other curves. C) Holocene SST signals from the Iberian Margin
615 using MAT based on planktonic foraminifera for cores MD99-2331 (after Naughton et al.,
616 2007b) and MD95-2042 (after Chabaud et al., 2014) and Alkenones for cores D13882 (after
617 Rodrigues et al., 2009) and MD01-2444 (after Martrat et al., 2007).

618

619 **Figure 4:** Comparison of annual SST Holocene signals from the Bay of Biscay (A and B)
620 with records from the northern North Atlantic highlighting variations of the NAC intensity
621 and SPG dynamics; C) SST signal of core MSM5/5-712-2 (Fram strait, Werner et al., 2013)
622 and of D) core M23258 (Barents shelf, after Sarnthein et al., 2003), both reconstructed using
623 the Modern Analog Technique (MAT) based on planktonic foraminifera; E) Concentration of
624 NAC indicator coccolith species in core MD99-2269 (North Iceland Shelf, after Giraudeau et
625 al., 2004) and in F) core B997-330 (North Iceland Shelf, after Andrews and Giraudeau, 2003);
626 The PP10-07 record is here also plotted by a thin dotted red line to underline the comparison;
627 G) Holocene Storm Periods (after Sorrel et al., 2012) reconstructed from sedimentological
628 evidence from a compilation of coastal cores in North-western Europe; H) core Rapid-12-1K
629 (Thornalley et al., 2009) proxy for upper-water column stratification, calculated using derived
630 Mg/Ca and $\delta^{18}\text{O}$ temperatures and salinities of *G. bulloides* and *G. inflata*. Dotted vertical
631 lines point out events of density anomalies at sub-thermocline depths in the southern Iceland
632 basin.

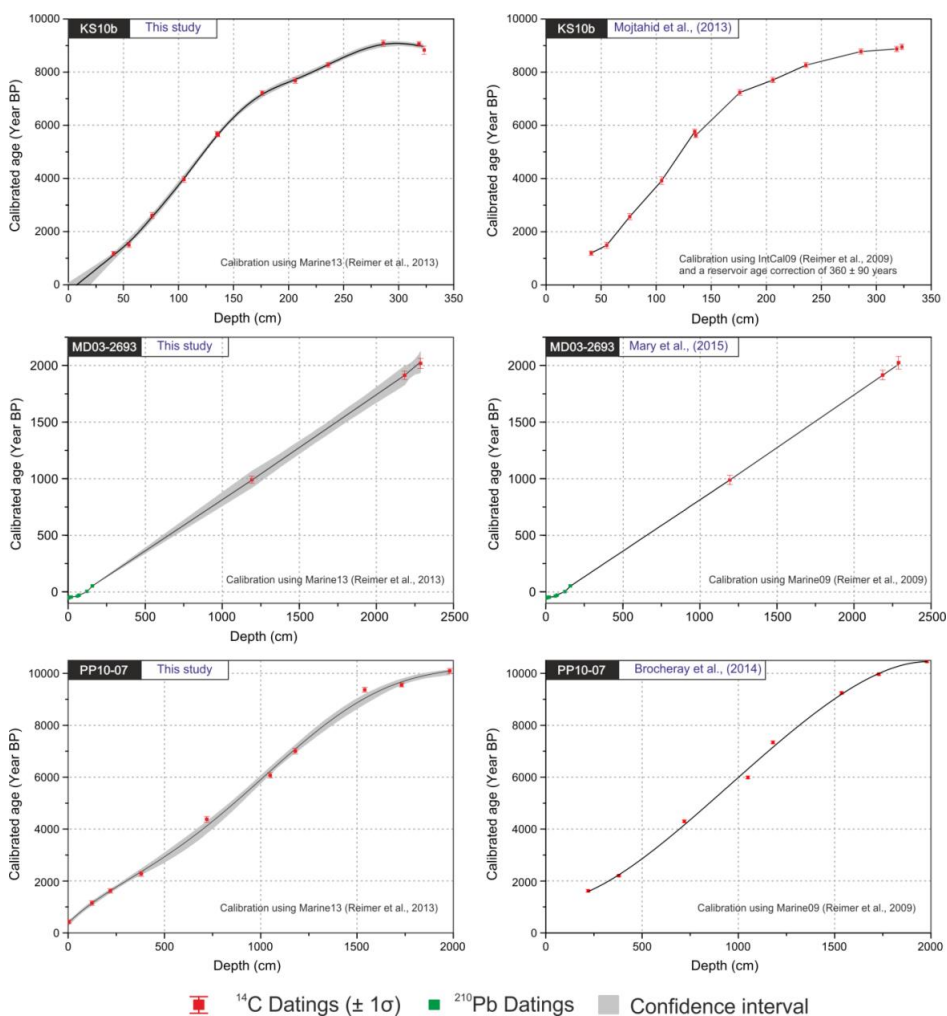
633 Changes in gyre circulation dynamics are compared with the Holocene division of Wanner et
634 al. (2008). The topmost arrows indicate periods of probable weak SPG also corresponding to
635 cold anomalies in the southern Bay of Biscay. Pink bands conversely highlight periods of
636 warmth which also correspond to enhanced NAC activity North of Iceland.

637



638
639

640 **Figure 1:** A) map showing the regional scheme of the main surface currents in the Bay of Biscay, drawn
 641 after the compilation of modern hydrological survey from Pingree and Garcia-Soto (2014). North Atlantic
 642 Current (NAC), Iberian poleward Current (IPC), and European Slope Current (ESC) are respectively
 643 represented by the red and orange arrows. The studied sedimentary cores PP10-07 and KS10b from the
 644 inner Bay of Biscay are shown in red. Additional Holocene records cited in the text are displayed by green
 645 squares. B) North Atlantic general circulation pattern (SPG: Subpolar Gyre, STG: Subtropical Gyre, EPC:
 646 European Poleward Current, after Lherminier and Thierry, 2015) with the location of the northern and
 647 southern sedimentary records discussed in the text. Core references: 1-Brocheray et al., 2014; 2-Mojtahid
 648 et al., 2013; 3-Gaudin et al., 2006; Mary et al., 2015; 4-Naughton et al., 2007a; 5-Pena et al., 2010; 6-
 649 Werner et al., 2013; 7-Sarnthein et al., 2003; 8-Giraudeau et al., 2004; 9-Andrews and Giraudeau, 2003;
 650 10-Thornalley et al., 2009; 11- Naughton et al., 2007b; 12-Abrantes et al., 2011; 13-Chabaud et al., 2014;
 651 14- Rodrigues et al., 2009; 15- Martrat et al., 2007.
 652



653

654

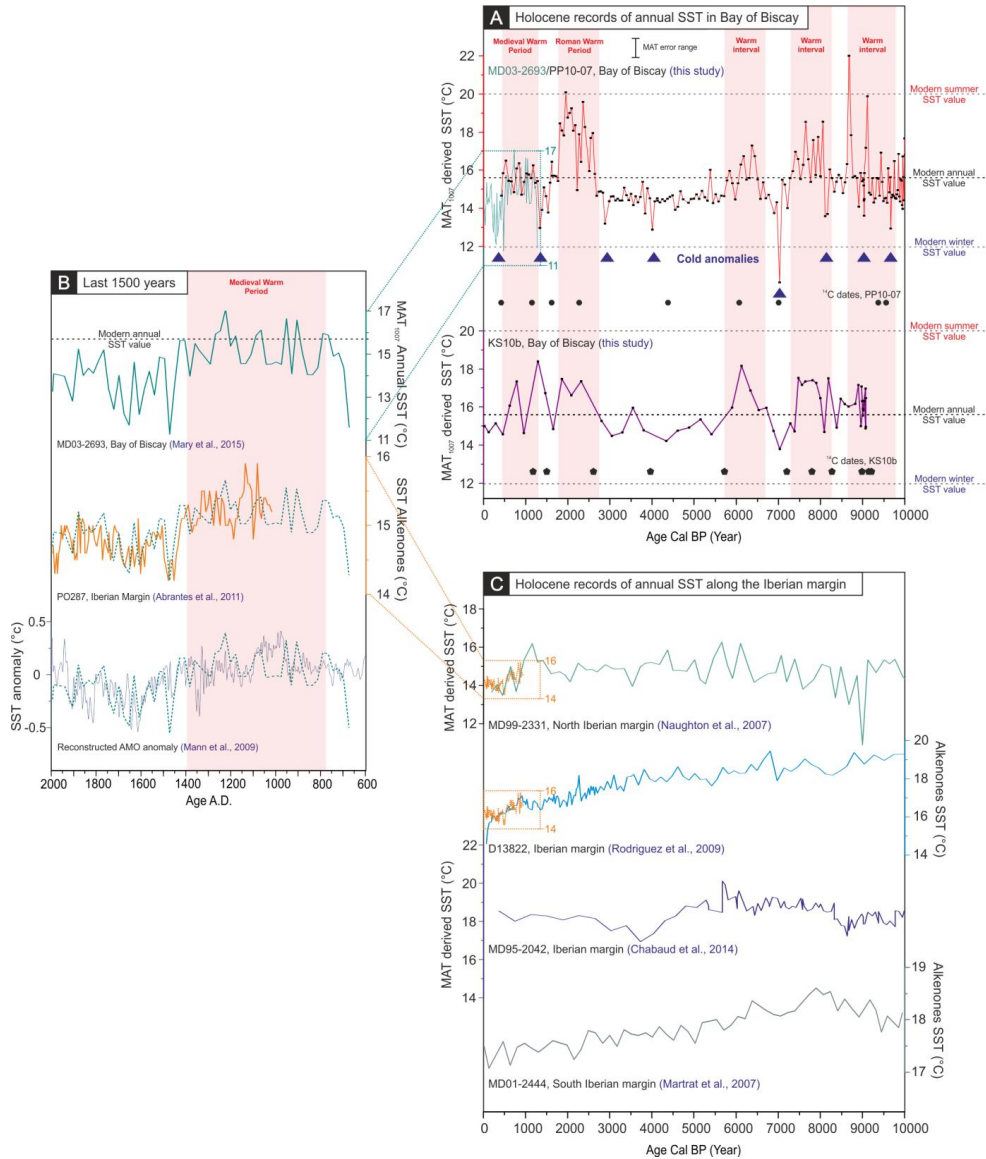
655

656

Figure 2: Revised age models for cores KS10b, MD03-2693, and PP10-07 (left panels) compared to previous published age models (right panels with original references).



657



658
659

660 **Figure 3:** Mean Annual sea surface temperature (SST) records from the Western European margin. A) Holocene SST
 661 signals from cores PP10-07 and KS10b (this study) reconstructed using the Modern Analog Technique (MAT) based on
 662 planktonic foraminifera (see Methods), and compared to SST signal of the adjacent core MD03-2693 (Mary et al., 2015).
 663 Black dots identify 14C age control points. B) SST signals spanning the last 1500 years in the Bay of Biscay (core MD03-
 664 2693) based on MAT and from the Iberian Margin (core P0287-06, Abrantes et al., 2011) using alkenones. Reconstructed
 665 signals are compared with the AMO reconstruction of Mann et al., (2009). The dotted curve represents core MD03-2693
 666 signal transposed on top of the two other curves. C) Holocene SST signals from the Iberian Margin using MAT based on
 667 planktonic foraminifera for cores MD99-2331 (after Naughton et al., 2007b) and MD95-2042 (after Chabaud et al., 2014)
 668 and Alkenones for cores D13882 (after Rodrigues et al., 2009) and MD01-2444 (after Martrat et al., 2007).

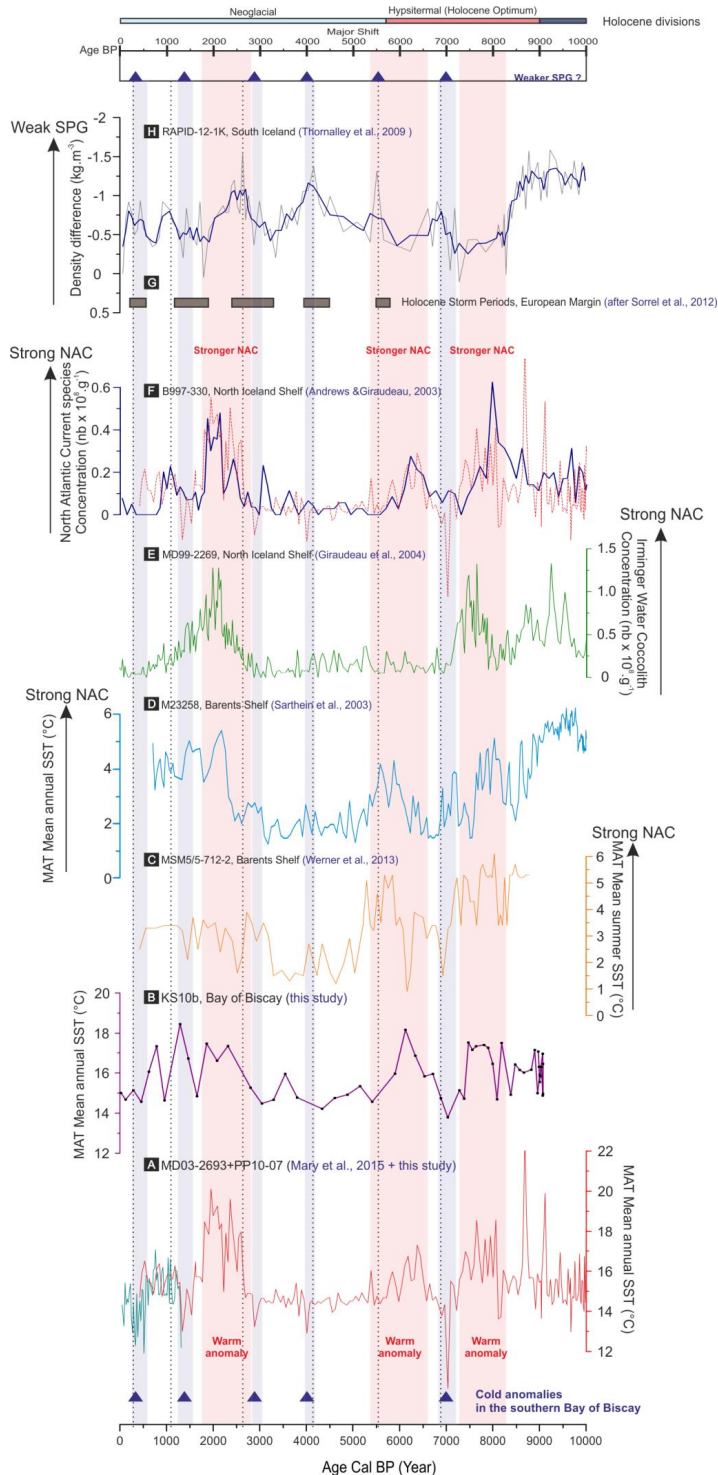


Figure 4: Comparison of annual SST Holocene signals from the Bay of Biscay (A and B) with records from the northern North Atlantic highlighting variations of the NAC intensity and SPG dynamics; C) SST signal of core MSM5/5-712-2 (Fram strait, Werner et al., 2013) and of D) core M23258 (Barents shelf, after Sarthein et al., 2003), both reconstructed using the Modern Analog Technique (MAT) based on planktonic foraminifera; E) Concentration of NAC indicator coccolith species in core MD99-2269 (North Iceland Shelf, after Giraudeau et al., 2004) and in F) core B997-330 (North Iceland Shelf, after Andrews and Giraudeau, 2003); The PP10-07 record is here also plotted by a thin dotted red line to underline the comparison; G) Holocene Storm Periods (after Sorrel et al., 2012) reconstructed from sedimentological evidence from a compilation of coastal cores in North-western Europe; H) core Rapid-12-1K (Thornalley et al., 2009) proxy for upper-water column stratification, calculated using derived Mg/Ca and $\delta^{18}\text{O}$ temperatures and salinities of *G. bulloides* and *G. inflata*. Dotted vertical lines point out events of density anomalies at sub-thermocline depths in the southern Iceland basin. Changes in gyre circulation dynamics are compared with the Holocene division of Wanner et al. (2008). The topmost arrows indicate periods of probable weak SPG also corresponding to cold anomalies in the southern Bay of Biscay. Pink bands conversely highlight periods of warmth which also correspond to enhanced NAC activity North of Iceland.